Resonances and Torsion Numbers of Driven Dissipative Nonlinear Oscillators

Ulrich Parlitz and Werner Lauterborn
Drittes Physikalisches Institut, Universität Göttingen

Z. Naturforsch. **41 a,** 605–614 (1986); received December 23, 1985

The torsion of the local flow around closed orbits and its relation to the superstructure in the bifurcation set of strictly dissipative nonlinear oscillators is investigated. The torsion number describing the twisting behaviour of the flow turns out to be a suitable invariant for the classification of local bifurcations and resonances in those systems. Furthermore, the notions of winding number and resonance are generalized to arbitrary one-dimensional dissipative oscillators.

I. Introduction

Recently we described the superstructure in the bifurcation set of the Duffing equation

$$\ddot{x} + d\dot{x} + x + x^3 = a\cos(\omega t) \tag{1}$$

and its relation to nonlinear resonances [1]. To give an intuitive understanding of these resonances and a motivation for our classification of the resonance horns in the phase diagrams, the Fourier spectra of periodic orbits were considered. A resonance horn occurs whenever a harmonic of the oscillation coincides with a certain eigenfrequency of the oscillator. The resonances are connected with deformations of the orbits, that can be described by a winding number given by the number of rotations of the tangent vector along the closed orbit*. Although being phenomenological, our concepts of eigenfrequencies and winding numbers enable a very fruitful discussion of the dynamical behaviour of nonlinear oscillators [1–4]. On the other hand the (orbit dependent!) eigenfrequency is not yet well defined for nonlinear systems and the winding numbers defined above are no topological invariants. Furthermore, with this heuristical interpretation of "resonance" it is not possible to explain the qualitative differences between odd and even resonances of symmetric and asymmetric oscillators (see Section IV).

Reprint requests to Prof. Dr. W. Lauterborn, Drittes Physikalisches Institut, Universität Göttingen, D-3400 Göttingen.

* This winding number is different from the winding number (or rotation number) usually defined in the context of phase locking oscillations (see Section VI).

These problems may be overcome by considering the nonlinear resonances in dissipative systems from a geometrical point of view, i.e. by investigating the twisting of the local flow around closed orbits. A quantity to described this property of the flow is the torsion number [5–11] that will be defined in Section II. Section III contains a brief discussion of the torsion number of the driven harmonic oscillator. It turned out that this analysis may help in understanding some features of the superstructure of nonlinear oscillators as discussed in Section IV.

Furthermore, the winding number in the classification scheme of resonances proposed in [1] is substituted by the torsion number. It is shown that this leads to a description with the desired invariance properties (Section V). Based on the concept of torsion numbers we define a new winding number for driven dissipative non-linear oscillators that does not require the existence of an invariant torus in phase space. This winding number enables an exact definition of "resonance" for those systems (Section VI).

II. Torsion Numbers

For a given periodic orbit nearby starting trajectories are more or less twisted around it [5–11]. Figure 1 shows typical situations. This twisting behaviour determines which bifurcations are possible. A torsion by 2π, for example, excludes period doubling because the eigenvalues of the linearization of the Poincaré map are positive. The torsion number of a periodic orbit is a quantity that counts the (average) number of twists of nearby trajectories

0340-4811 / 86 / 0400-0605 $ 01.30/0. – Please order a reprint rather than making your own copy.

around the closed orbit. We shall make these ideas more precise now and give a definition for the torsion number of periodic orbits. In the following we will consider systems of the type

$$\ddot{x} + g(x, \dot{x}) = h(t) \quad \Leftrightarrow \quad \begin{aligned} \dot{x}_1 &= x_2, \\ \dot{x}_2 &= -g(x_1, x_2) + h(Tx_3), \\ \dot{x}_3 &= 1/T = \omega/2\pi, \end{aligned} \tag{2}$$

where $h(t+T) = h(t)$.

Such systems generate a flow $\Phi = \{\Phi^t\}$ on the phase space $\mathbb{R}^2 \times S^1$. Equation (2, right) can be written in a concise form as $\dot{\boldsymbol{x}} = V(\boldsymbol{x})$, where V is the vector field. The Poincaré map $P = \Phi^T|_\Sigma$ is defined on the cross section

$$\Sigma = \{(x_1, x_2, x_3) \in \mathbb{R}^2 \times S^1 : x_3 = c = \text{const}\} \cong \mathbb{R}^2.$$

Let γ be a period-m orbit through

$$\boldsymbol{x}^* = (x_{1f}, x_{2f}, x_{3f} = c) \in \mathbb{R}^2 \times S^1$$

described by a solution $x(t)$ of (2, left) and let $\boldsymbol{x}_f = (x_{1f}, x_{2f}) \in \mathbb{R}^2$ be a fixed point of P^m associated with the period-m orbit γ we want to investigate. The evolution of a nearby trajectory starting at $\boldsymbol{x}_0 = \boldsymbol{x}_f + \boldsymbol{y}_0$ is given by the derivative DV of the vector field V:

$$\dot{\boldsymbol{x}} + \dot{\boldsymbol{y}} = V(\boldsymbol{x} + \boldsymbol{y}) = V(\boldsymbol{x}) + DV(\boldsymbol{x})\,\boldsymbol{y} + \ldots$$

or for small perturbations ($\boldsymbol{y} \to 0$):

$$\dot{\boldsymbol{y}} = DV(\boldsymbol{x})\,\boldsymbol{y} \tag{3}$$

with

$$DV(\boldsymbol{x}) = \begin{pmatrix} 0 & 1 & 0 \\ -\dfrac{\partial g}{\partial x_1}(x_1, x_2) & -\dfrac{\partial g}{\partial x_2}(x_1\ x_2) & \dfrac{\partial h}{\partial x_3} \\ 0 & 0 & 0 \end{pmatrix}.$$

Since the third component of (3) has a trivial solution $y_3 = \text{const}$, (3) may be reduced to a two-dimensional system of differential equations. If $\boldsymbol{x}_0$ is restricted to $\Sigma = \{x \in \mathbb{R}^2 \times S^1 : x_3 = 0\}$ (i.e., $\boldsymbol{y}_0 = (y_{10}, y_{20}, 0)$) this reduced variational equation is given by

$$\ddot{y} + \frac{\partial g}{\partial \dot{x}}(x, \dot{x})\,\dot{y} + \frac{\partial g}{\partial x}(x, \dot{x})\,y = 0$$

$$\Leftrightarrow \quad \begin{aligned} \dot{y}_1 &= y_2, \\ \dot{y}_2 &= -\frac{\partial g}{\partial x} y_1 - \frac{\partial g}{\partial \dot{x}} y_2. \end{aligned} \tag{4}$$

Any solution $\boldsymbol{u}(t) = (u_1(t), u_2(t))$ of (4, right) describes a spiral-like curve in the phase space $\{(y, \dot{y})\}$ (compare Figure 1 c). The number of torsions can be counted by:

– considering $\boldsymbol{u} = (u_1, u_2)$ in polar coordinates (r, β)

$$\cos\beta = \frac{u_2}{r}, \quad \sin\beta = \frac{u_1}{r}, \quad r = \sqrt{u_1^2 + u_2^2}$$

– computing the angular velocity

$$\dot{\beta}(t) = \frac{\dfrac{\mathrm{d}}{\mathrm{d}t}\sin\beta}{\cos\beta} = \frac{u_1 \dot{u}_2 - \dot{u}_1 u_2}{u_1^2 + u_2^2}$$

– determining the average angular velocity

$$\Omega(\gamma) := \lim_{t \to \infty} \frac{1}{t} \left| \int_0^t \dot{\beta}(t')\,\mathrm{d}t' \right|.$$

– and counting the number of torsions during one period $T_m = m\,T = m\,\dfrac{2\pi}{\omega}$ of the oscillation:

$$n = \frac{T_m}{2\pi}\,\Omega(\gamma) = \frac{\Omega(\gamma)}{\omega_m} = m\,\frac{\Omega(\gamma)}{\omega}.$$

The torsion number n of a period-m-orbit is therefore defined by

$$n = m\,\frac{\Omega(\gamma)}{\omega}, \tag{5}$$

where

$$\Omega(\gamma) = \lim_{t \to \infty} \frac{1}{t} \left| \int_0^t \frac{u_1 \dot{u}_2 - \dot{u}_1 u_2}{u_1^2 + u_2^2}\,\mathrm{d}t \right|.$$

$\Omega(\gamma)$ is independent of the initial condition $\boldsymbol{u}(0)$ of the solution $\boldsymbol{u}(t)$ of the variational equation (4, right) and may be viewed as the orbit dependent eigenfrequency of the oscillator (2). If $\lambda_{1,2} = r\,e^{\pm i\varphi}$, $r > 0$, are complex eigenvalues of the derivative DP^m of the iterated Poincaré map P^m (or the Floquet multipliers) then the phase factor φ is given by $\varphi = T_m \cdot \Omega(\gamma) \bmod 2\pi$.

Our torsion number is measured in units of 2π, while giving the formula (6) for the torsion number N_k of a period doubling orbit just before the k-th bifurcation Beiersdorfer [10] counts rotations of the invariant manifolds by π. Thus according to our definition N_k must be replaced by $n_k = N_k/2$ in

$$N_k = \tfrac{1}{3}\left((3N_0 + 2)\,2^{k-1} + (-1)^{k-1}\right) \tag{6}$$

(N_0 is the number of torsions of the first attractor in the cascade, see [10]).

In the following the torsion number n and the period m will be used to label the resonances $R_{n,m}$ of nonlinear oscillators. In Sect. V we come back to the problem of classification of resonances and bifurcations and give arguments in favour of this procedure.

A relation exists between the torsion of the local flow and the Lyapunov spectrum. Instead of a single trajectory in the neighbourhood of the closed orbit γ a small volume following the orbit may be considered. The deformation of this volume (independent of its orientation!) is given by the Lyapunov characteristic exponents (see e.g. [12]). The volume, however, also rotates around the orbit γ during its flight along γ. As shown below the average rotational frequency about the tangent vector is given by $\Omega(\gamma)$. To elucidate this connection between the torsion and the Lyapunov spectrum a further derivation of (5) is given using the QR-decomposition of the linearized flow map $D\Phi^t$ [12]. Each invertible $n \times n$-matrix A can be splitted uniquely into the product of an orthogonal matrix Q and an upper triangular matrix R with non-negative diagonal elements. For the 2×2 case with $\det(A) > 0$ the matrices Q and R are:

$$\begin{pmatrix} a & b \\ c & d \end{pmatrix} = A = Q \cdot R = \begin{pmatrix} \cos\alpha & -\sin\alpha \\ \sin\alpha & \cos\alpha \end{pmatrix} \cdot \begin{pmatrix} r_{11} & r_{12} \\ 0 & r_{22} \end{pmatrix}$$

with

$$\cos\alpha = \frac{a}{\sqrt{a^2+c^2}}, \quad r_{11} = \sqrt{a^2+c^2}, \quad r_{22} = \frac{ad-bc}{\sqrt{a^2+c^2}},$$

$$\sin\alpha = \frac{c}{\sqrt{a^2+c^2}}, \quad r_{12} = \frac{ba+cd}{\sqrt{a^2+c^2}}.$$

We are interested in the rotations of the volume about the (timedependent) axis given by the tangent vector of the trajectory. The number of these rotations equals the number of rotations of the projection of the volume onto the $y_1 - y_2$-plane (see Figure 1). Therefore we can simplify the discussion by considering only the first two coordinates of the linearized flow map $D\Phi^t$, i.e. by considering the 2×2-matrix $A(t) = D\Phi^t|_{\mathbb{R}^2} = Q(t)\,R(t)$ (compare Equation (4)). The matrix R contains the information of the nontrivial values of the Lyapunov spectrum [12], whereas Q describes the rotation of the small volume. The (timedependent) rotational velocity $\dot{\alpha}$ of the volume is given by

$$\dot{\alpha}(t) = \frac{\frac{\mathrm{d}}{\mathrm{d}t}\sin\alpha}{\cos\alpha} = \frac{\dot{c}(t)\,a(t) - \dot{a}(t)\,c(t)}{a(t)^2 + c(t)^2}.$$

The components $a(t)$ and $c(t)$ of $A(t)$ are the solutions $u_1(t)$ and $u_2(t)$ of the variational equation (4) with the initial values $u_1(0) = 1$ and $u_2(0) = 0$. Thus we obtain for $\dot{\alpha}$ the integrand of (5)

$$\dot{\alpha}(t) = \frac{\dot{u}_2\,u_1 - u_2\,\dot{u}_1}{u_1^2 + u_2^2}.$$

This simple example shows that some information about "resonance" is contained in the orthogonal part $Q(t)$ of the linearized flow map $D\Phi^t = Q(t)R(t)$. In higher dimensional systems a small test-volume possesses more rotational degrees of freedom and thus a whole spectrum of eigen- or torsionfrequencies $\Omega_i(\gamma)$ exists. These ideas will be discussed in detail elsewhere.

III. Torsion Numbers of the Harmonic Oscillator

As a first example we compute the torsion numbers of the driven harmonic oscillator

$$\ddot{x} + \mathrm{d}\dot{x} + \omega_0^2 x = a\cos(\omega t). \tag{7}$$

All solutions of (7) converge asymptotically to the only periodic solution

$$x_{\mathrm{inh}}(t) = \frac{a}{\sqrt{(\omega_0^2 - \omega^2)^2 + d^2\omega^2}}\cos(\omega t - q), \tag{8}$$

$$q = \operatorname{arccot}\left(\frac{\omega_0^2 - \omega^2}{\mathrm{d}\omega}\right).$$

Hence the Poincaré map of this system has a single stable fixed point $\boldsymbol{x}_{\mathrm{f}}$. The evolution of a perturbation (initial value in the Poincaré cross section located at $x_3 = 0 = t$: $\boldsymbol{x}_{\mathrm{p}} = \boldsymbol{x}_{\mathrm{f}} + (y_0, \dot{y}_0)$) describing the behaviour of a trajectory in the neighbourhood of the closed orbit is given by the variational equation

$$\ddot{y} + \mathrm{d}\dot{y} + \omega_0^2 y = 0. \tag{9}$$

For $d < 2\omega_0$ the solution of (9) is

$$y(t) = e^{-\frac{1}{2}\mathrm{d}t}\left(y_0\cos(\tilde{\omega}t) + \frac{\dot{y}_0 + \frac{1}{2}d\,y_0}{\tilde{\omega}}\sin(\tilde{\omega}t)\right)$$

$$\tilde{\omega} = \sqrt{\omega_0^2 - \tfrac{1}{4}d^2}. \tag{10}$$

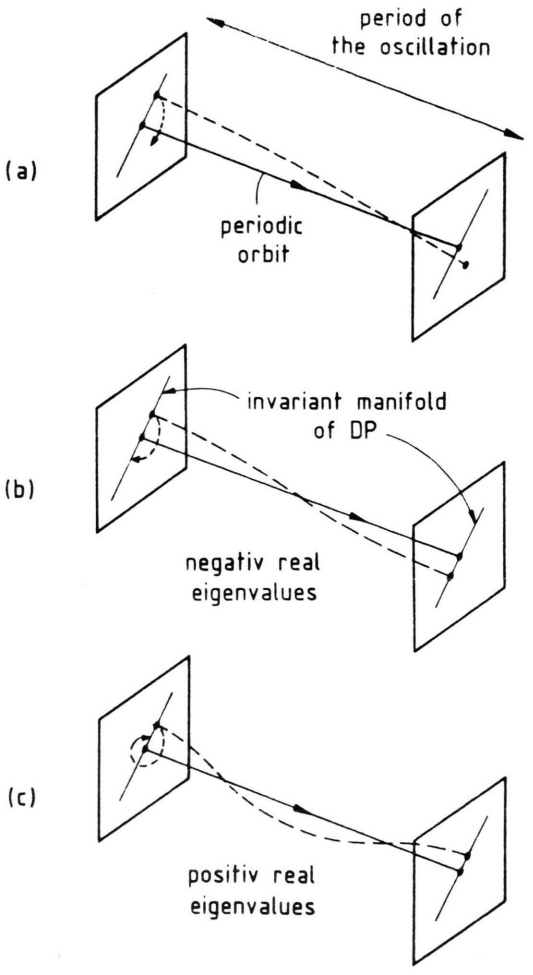

Fig. 1. The torsion of the local flow (represented by the dashed trajectory) around a periodic orbit (symbolized by the straight line). When a nearby trajectory is twisted around the closed orbit by an integer multiple of π the derivative of the Poincaré map DP has negative (b) or positive (c) real eigenvalues.

The frequency $\tilde{\omega}$ of the oscillations of the perturbation is independent of the excitation frequency ω and the excitation amplitude a. The rotation angle of the neighbour trajectory around the closed orbit depends only on the frequency relation $\tilde{\omega}/\omega$.

If the angle is a multiple of π $\boldsymbol{x}_p$ lies in an eigenspace of the derivative DP of the Poincaré map P (compare Figure 1). This can also be seen by the following analysis. From (10) an explicit expression for the Poincaré map P can be derived.

$$P\colon \mathbb{R}^2 \to \mathbb{R}^2$$
$$\boldsymbol{x} \mapsto P(\boldsymbol{x}) = \boldsymbol{x}_f + DP(\boldsymbol{x}_f)(\boldsymbol{x} - \boldsymbol{x}_f),$$

where

$$DP(\boldsymbol{x}) = DP = \exp\left\{\left(-\frac{d}{2} + i\tilde{\omega}\right)\frac{2\pi}{\omega}\right\}\begin{pmatrix} a & b \\ a\bar{a} & \bar{a} \\ b & \end{pmatrix} + cc,$$

$$a := \frac{1}{2} - i\frac{d}{4\tilde{\omega}}, \quad b := -\frac{i}{2\tilde{\omega}}.$$

The eigenvalues $\lambda_{1,2}$ of DP for $d < 2\omega_0$ are given by

$$\lambda_{1,2} = e^{-\frac{d\pi}{\omega}}\left[\cos\left(2\pi\frac{\tilde{\omega}}{\omega}\right) \pm i\sin\left(2\pi\frac{\tilde{\omega}}{\omega}\right)\right]. \tag{11}$$

For real eigenvalues the real eigenvectors rotate an integer multiple of π around the closed orbit during one period of the excitation (see Figure 1). The imaginary parts $\mathrm{Im}(\lambda_i)$ vanish for

$$\omega = \frac{2}{N}\tilde{\omega}, \quad N = 1, 2, 3, \ldots.$$

The torsion number is given by $n = \tilde{\omega}/\omega$. The first integer torsion number $n = 1$ (i.e. the second zero of $\mathrm{Im}(\lambda_i)$ $(N = 2)$) appears at $\tilde{\omega} = \omega$ between the ordinary velocity- and amplitude resonances ($\omega_v = \omega_0$, $\omega_a = \sqrt{\omega_0^2 - \frac{1}{2}d^2}$) of the linear oscillator.

For $d \geqq 2\omega_0$ the eigenvalues are given by

$$\lambda_{1,2} = e^{-\frac{d\pi}{\omega}}\left[-\frac{g(\omega^*/\omega)}{2} \pm \sqrt{\tfrac{1}{4}g^2 - 1}\right], \tag{12}$$

$$g(\omega^*/\omega) = e^{2\pi\frac{\omega^*}{\omega}} + e^{-2\pi\frac{\omega^*}{\omega}}, \quad \omega^* := \sqrt{\tfrac{1}{4}d^2 - \omega_0^2}. \tag{12}$$

All λ_i are real, and the eigenspaces do not rotate around the closed orbit. The torsion number is always zero.

IV. Torsion Numbers of Nonlinear Oscillators

The twisting behaviour of the flow around closed orbits described above is strongly related to the resonances and the superstructure in the bifurcation set of nonlinear oscillators. To show this we discuss two examples, the asymmetric Toda oscillator and the symmetric Duffing equation (1).

(a) Oscillators with Asymmetric Potentials

A very simple asymmetric oscillator, i.e. an oscillator with asymmetric potential, is the Toda

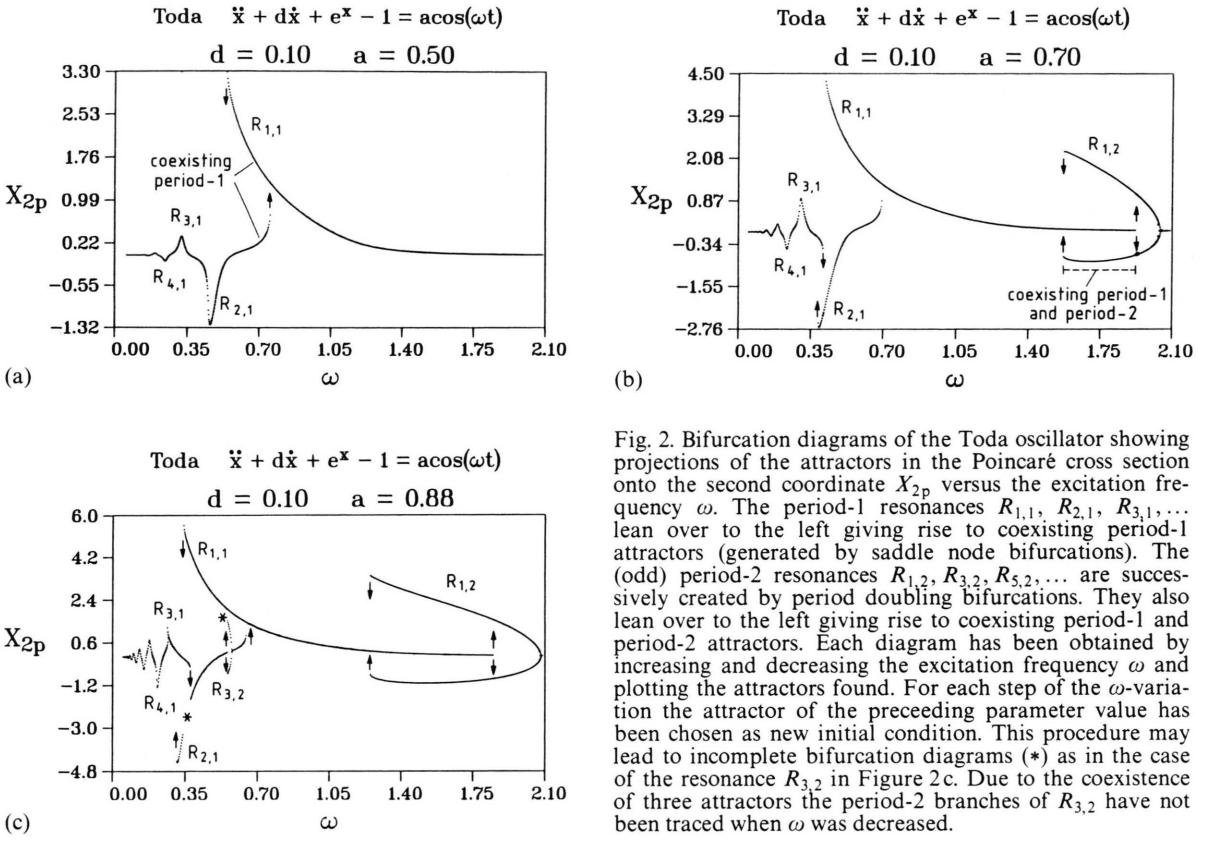

Fig. 2. Bifurcation diagrams of the Toda oscillator showing projections of the attractors in the Poincaré cross section onto the second coordinate X_{2p} versus the excitation frequency ω. The period-1 resonances $R_{1,1}$, $R_{2,1}$, $R_{3,1}$, ... lean over to the left giving rise to coexisting period-1 attractors (generated by saddle node bifurcations). The (odd) period-2 resonances $R_{1,2}$, $R_{3,2}$, $R_{5,2}$, ... are successively created by period doubling bifurcations. They also lean over to the left giving rise to coexisting period-1 and period-2 attractors. Each diagram has been obtained by increasing and decreasing the excitation frequency ω and plotting the attractors found. For each step of the ω-variation the attractor of the preceeding parameter value has been chosen as new initial condition. This procedure may lead to incomplete bifurcation diagrams (*) as in the case of the resonance $R_{3,2}$ in Figure 2c. Due to the coexistence of three attractors the period-2 branches of $R_{3,2}$ have not been traced when ω was decreased.

oscillator (for more details see [4])

$$\ddot{x} + d\dot{x} + e^x - 1 = a\cos(\omega t). \tag{13}$$

Typical ω-bifurcation diagrams for three different excitation amplitudes $a = 0.5$, $a = 0.7$ and $a = 0.88$ and fixed damping $d = 0.1$ are shown in Figure 2. For successively increased excitation amplitudes a the period-1 resonances $R_{1,1}$ (main resonance), $R_{2,1}, R_{3,1}, \ldots$ become steeper and steeper and then lean over to the left. In contrast to this the period-2 resonances $R_{1,2}, R_{3,2}, R_{5,2}, \ldots$ occur "suddenly" by a period doubling bifurcation. This alternating resonance scenario can be explained by the eigenvalue evolution (of the harmonic oscillator). Again we have to consider the variational equation around the closed orbit γ, that is described by the solution $x(t)$ of (13)

$$\ddot{y} + d\dot{y} + e^x y = 0 \tag{14}$$

and the eigenvalues of the derivative DP of the Poincaré map P which is now calculated numerically (see [10] for details). For sufficiently small a, i.e. also small amplitudes of the oscillation x, we have nearly the same eigenvalues as in the linear case (11). Figure 3 shows the eigenvalue evolution of the Toda oscillator corresponding to the bifurcation diagram in Figure 2a. In contrast to the linear case there are small ω-intervals where the eigenvalues become real. With increasing excitation amplitude a one of these two real eigenvalues tends to the critical values $+1$ or -1.

Touching $+1$ leads to saddle node bifurcations and the leaning over of the period-1 resonances $R_{n,1}$. Whenever a real eigenvalue reaches -1 a period doubling bifurcation takes place, creating a period-2 resonance $R_{n,2}$. Thus the excitation of nonlinear resonances and the difference between period-1 and period-2 resonances can be explained

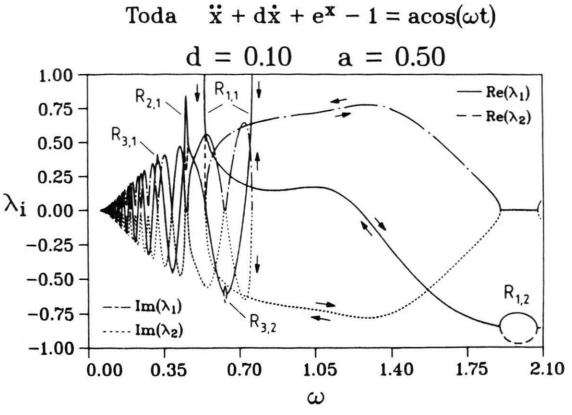

Fig. 3. Eigenvalue evolution of DP corresponding to the bifurcation diagram given in Figure 2a. When the excitation amplitude a is increased more and more the "bubbles" where two real eigenvalues appear ($R_{1,2}$, $R_{3,2}$) will touch -1 and period doubling bifurcations creating the period-2 resonances will take place (see Fig. 2b, c and Table 1). The coming bifurcations are announced in this plot. Where the curves touch $+1$ saddle node bifurcations occur.

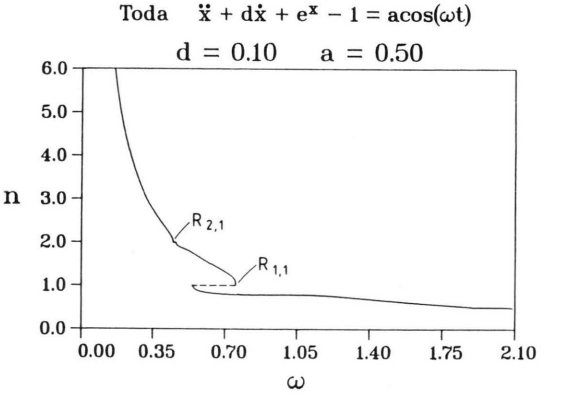

Fig. 4. The torsion number n versus the excitation frequency ω. At the plateaus around saddle node bifurcation values of ω the torsion number n equals integers (see Section V).

by the torsion of the flow which is determined by the linear limit case. Figure 4 shows the increase of the torsion number n for small ω. The same results have recently been obtained for the model of bubble oscillations given in [2].

(b) Oscillators with Symmetric Potentials

An example for a symmetric system is Duffing's equation (1). The symmetry of the vector field V ($V(x_1, x_2, x_3) = -V(-x_1, -x_2, x_3 + \frac{1}{2})$ implies the existence of a root $-\tilde{P}$ of the Poincaré map $P = (-\tilde{P})^2$, where $\tilde{P} := \Phi^{T/2}|_\Sigma$ [13]. Figure 5a shows a typical bifurcation diagram of Duffing's equation for a medium excitation amplitude a. In contrast to the Toda oscillator symmetry bifurcations (i.e. saddle node bifurcations creating two asymmetric period-1-orbits) occur between the resonances $R_{1,1}, R_{3,1}, R_{5,1} \ldots$ when the excitation amplitude a is increased [1]. The first symmetry breaking appears at the left hand side of $R_{1,1}$ (while the first period doubling in Fig. 2b occurs at the right of $R_{1,1}$). Figures 5b and 5c show the evolution of the eigenvalues of the linearization DP and the torsion number in dependence on the control parameter ω, respectively.

To understand the different behaviour of the symmetric and the asymmetric system we have to consider the Poincaré map P_T of the Toda oscillator and the root $-\tilde{P}_D$ of the Poincaré map P_D of the Duffing oscillator. As shown in Fig. 6, the eigenvalues of $\tilde{P}_D$ evolve similar to those of the Toda oscillator (Figure 3). The different bifurcation scenarios may thus be explained by the different signs of the derivatives DP_T and DP_D and their eigenvalues. The connection is given in Table 1 where both oscillators are compared in terms of the Toda Poincaré map P_T and the negative root $\tilde{P}_D$ of the Duffing Poincaré map P_D. The abbreviations are pd for period doupling, sn for (ordinary) saddle node bifurcations and sb for symmetry breaking.

Table 1. Torsion numbers, eigenvalues and bifurcations.

Torsion angle	5π	4π	3π	2π	π
Torsion number (5)	$2\frac{1}{2}$	2	$1\frac{1}{2}$	1	$\frac{1}{2}$
Toda oscillator (13)					
Eigenvalues of DP_T	neg.	pos.	neg.	pos.	neg.
Bifurcations	pd	sn	pd	sn	pd
Pictograms *Toda*	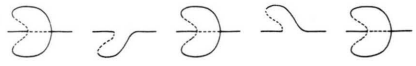				
Duffing oscillator (1)					
Eigenvalues of $D\tilde{P}_D$	neg.	pos.	neg.	pos.	neg.
Eigenvalues of $-D\tilde{P}_D$	pos.	neg.	pos.	neg.	pos.
Eigenvalues of $DP_D = (-D\tilde{P}_D)^2$	pos.	pos.	pos.	pos.	pos.
Bifurcations	sn	sb	sn	sb	sn
Pictograms *Duffing*					

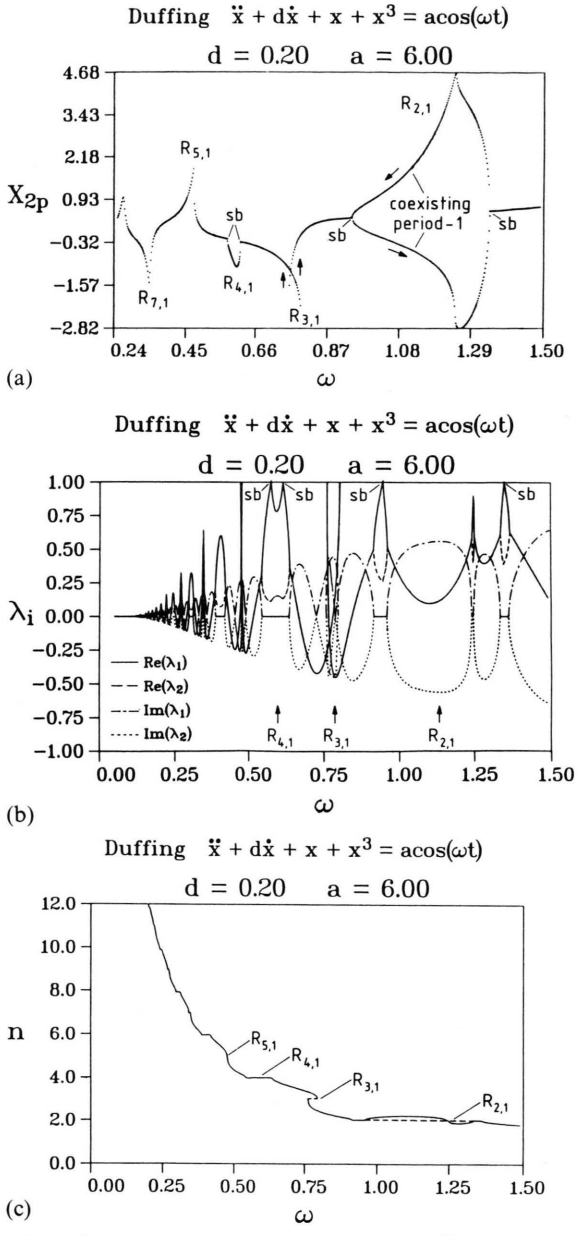

Fig. 5. (a) Bifurcation diagram of the Duffing oscillator (see also Fig. 2 and [1]). In contrast to the Toda oscillator no period doubling but symmetry bifurcations occur, the first being located between $R_{3,1}$ and $R_{1,1}$. ($R_{1,1}$ not shown in this plot.) The two branches of symmetry broken solutions the system follows for increasing and decreasing ω are denoted by arrows. The behaviour of the system at the symmetry bifurcation points (i.e. the choice of the branch) depends on the step size of the parameter variation, the basin structure of the two partner orbits being created and the errors of the numerical integration. (Compare $R_{2,1}$ and $R_{4,1}$.) – (b) Eigenvalue evolution corresponding to Figure 5a. – (c) Torsion number n versus ω corresponding to Fig. 5a (compare Figure 3).

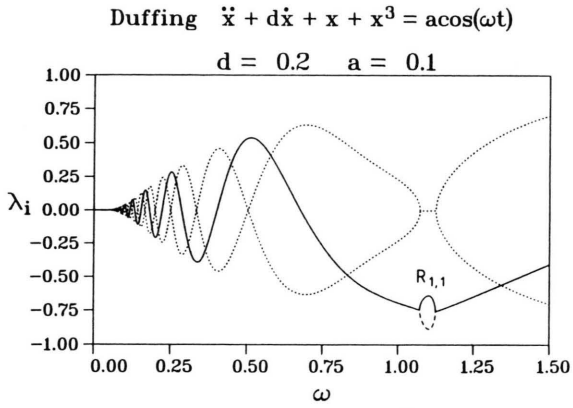

Fig. 6. Eigenvalues of the derivative $D\tilde{P}_D$ of the negative root $\tilde{P}_D$ of the Duffing Poincaré map $P_D = (-\tilde{P}_D)^2$ versus ω. Shown is the situation for very small excitation amplitudes (here $a = 0.1$) where the main resonance $R_{1,1}$ does not yet lean over. When the excitation amplitude a is increased the bubble $R_{1,1}$ will touch -1 and a saddle node bifurcation for P_D(!) takes place.

V. Classification of Resonance Horns and Local Bifurcations

The torsion number will now be used for the classification of resonances and local bifurcations in strictly dissipative one-dimensional oscillators. We call an oscillator strictly dissipative (or passive) if the associated Poincaré map P is area contracting everywhere on the cross section (i.e. $\forall x \in \Sigma$: $\det(DP(x)) < 1$). Examples for such systems are the Toda and the Duffing oscillator (for both we have $\det(DP) = \exp\{-2\pi d/\omega\} < 1$) and the bubble oscillator [2]. In these systems no Hopf bifurcations can occur. The assumption of a complex eigenvalue $\lambda = a + ib$ crossing the unit circle $|\lambda| = 1$ leads to the contradiction $1 = |\lambda|^2 = a^2 + b^2 = \lambda\bar{\lambda} = \det(DP) < 1$. Thus the eigenvalues of the derivative DP of the Poincaré map P must become real in the vicinity of parameter values where local bifurcations take place. Positive real eigenvalues leading to saddle node bifurcations are associated with integer torsion numbers. Every period doubling bifurcation ($\lambda_i = -1$) may be viewed as a saddle node bifurcation of the orbit with the double period. So in strictly dissipative systems an integer torsion number is uniquely related to every bifurcation point in the parameter space. Staying integers these numbers cannot change along bifurcation surfaces! Together with the period they are used to label the bifurca-

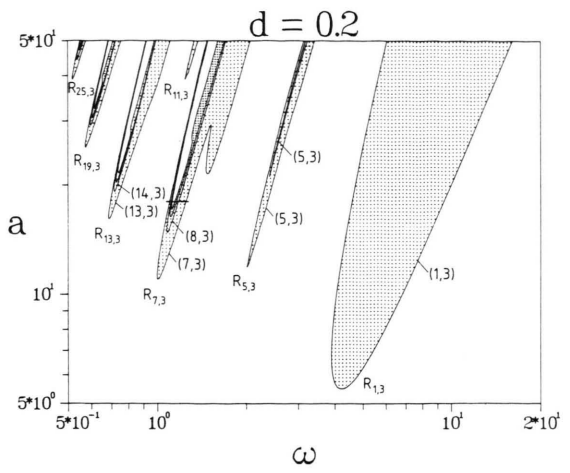

Fig. 7. Phase diagram of (coexisting) period-$3 \cdot 2n$ attractors of the Duffing equation (1). The bifurcation curves are labeled by the torsion number n and the period m as (n, m). The horizontal line through the horn $R_{7,3}$ gives the location of the bifurcation diagram shown in Figure 8.

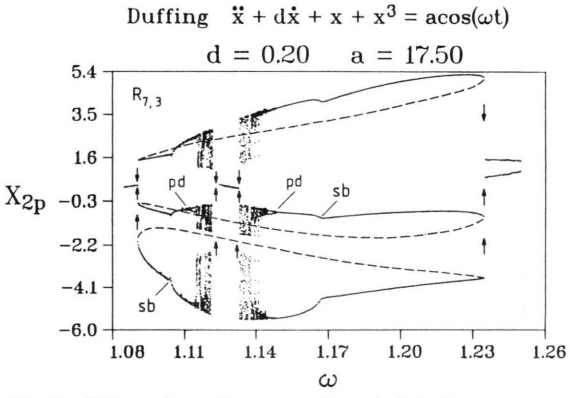

Fig. 8. Bifurcation diagram of period-$3 \cdot 2n$ attractors. Period doubling (pd) is again preceeded by symmetry breaking (sb). As in the case of the chaotic regime arising from the period-1 attractors, there is a gap in the chaotic band [1]. The dashed lines give the location of the unstable period-3 orbit being created at the boundary of the resonance horn (Fig. 7) by saddle node bifurcations. The torsion number of this unstable orbit is used to label the resonance horn $R_{7,3}$ of the phase diagram in Figure 7. To avoid incompleteness as discussed in connection with Fig. 2 the different branches have been traced independently.

tion curves in the phase diagrams. Figure 7 shows as an example the phase diagram of (coexisting, see [1]) period-$3 \cdot 2n$ attractors of Duffing's equation (1). To illustrate the meaning of the different bifurcation curves a bifurcation diagram of period-$3 \cdot 2n$ attractors is given in Figure 8. The resonance horns in Fig. 7 are labelled by the torsion number n and the period number m of the unstable period-3 orbits being created by saddle node bifurcations at the boundaries of the resonance horns (dashed curve in Figure 8). Analogous to the period-1 case illustrated in Table 1 (see Sect. IV) these (ordinary) saddle node bifurcations belong to odd torsion numbers. Saddle node bifurcations associated to odd torsion numbers being a multiple of three have not been found. For the damping value of $d = 0.2$ no symmetry bifurcations and period doublings occur inside the resonance horn $R_{1,3}$ in Figure 7.

It is easy to see that in strictly dissipative one dimensional oscillators the torsion number and the period of unstable periodic orbits remain invariant under parameter variation until the orbit becomes stable or vanishes by a saddle node bifurcation. The classification of the resonance horns given above is thus unique. Like the classification of the local bifurcations it allows the comparison of periodic orbits and their bifurcations in different parts of the parameter space.

VI. Resonances and Winding Numbers

Although resonance is an important feature of (driven) dissipative nonlinear oscillators there exists no exact mathematical definition of "resonance" for those systems. A definition can be given for integrable Hamiltonian Systems and systems where the phase space consists of a torus [14]. In these cases the angle variables or torus frequencies are used to define resonance as rational frequency relation between them. These ideas may be carried over to dissipative oscillators using the eigenfrequency $\Omega(\gamma)$ (5) of a given orbit γ that was defined in Section II. We introduce the frequency ratio

$$w(\gamma) = \frac{\Omega(\gamma)}{\omega} \quad [\Omega(\gamma) \text{ see (5)}]$$

and call it the *winding number* of the orbit γ.

This winding number is defined in the spirit of the rotation number*, but it depends on the orbit γ whereas the rotation number is a property of the whole system. This feature of the winding number enables the description of systems with coexisting

* The rotation number is often called winding number, too. We suggest to use the term winding number only in connection with the linearization approach given in Section II.

attractors. Furthermore, in contrast to the rotation number our winding number is well defined even in those cases where no invariant torus in the phase space exists (e.g. Duffing, Toda, ...). In the spirit of the existing resonance conditions [14] we call an orbit γ *resonant* when its winding number is rational. This definition is in good agreement with the classification of the resonance horns given in Section V.

VII. Winding Numbers of Strange Attractors

The above defined winding number is a quantity that is associated to a single orbit. It is an open question whether strange attractors possess well defined winding numbers, too. To investigate this problem we computed the winding number of orbits that belong to the strange attractors shown in Figure 8. The numerical results are given in Figure 9. According to (6) the period doubling cascade leads to steps in the winding number diagram. As w converges very badly for chaotic oscillations (the run for Fig. 9 took 350 hours cpu-time on a VAX 11/780!) this diagram should be viewed as a preliminary result. But also investigations of the Henon map that are presently done lead to similar diagrams. Winding numbers of strange attractors are a new and open field for both analytical and numerical work.

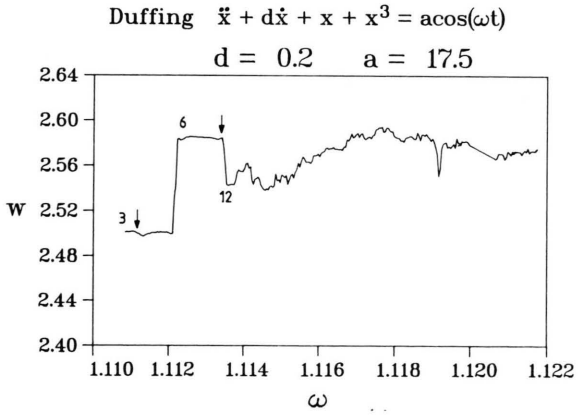

Fig. 9. Winding number diagram of the left period-$3 \cdot 2^n$-cascade into chaos shown in Figure 8. The steps denoted by the period number follow (6). The arrows indicate the bifurcation values.

VIII. Conclusion

The torsion number originally introduced by Beiersdorfer [9, 10], Uezu and Aizawa [6, 7] to describe the universal change in the topology of the invariant manifolds of period doupling orbits can also be used to understand, describe and classify resonances and local bifurcations in strictly dissipative oscillators. Thereby the concept of "the" eigenfrequency of an oscillator being well defined for linear oscillators and free oscillations of nonlinear oscillators (where it becomes amplitude dependent) has been extended to the driven case. In this way the notion of "resonance" up to now only loosely defined can be made more precise. The information about the torsion is contained in the orthogonal part of the QR-decomposition of the linearized flow map $D\Phi^t$. This result has been obtained for 3-dim systems on $\mathbb{R}^2 \times S^1$, but a generalization of the ideas presented in this paper to higher dimensional systems should be possible.

The consideration of the torsion of the local flow around periodic orbits has improved our understanding of the qualitative differences between odd and even resonances of symmetric and asymmetric oscillators. This torsion is already present in the case of the harmonic oscillator. Therefore, we conjecture that all driven nonlinear oscillators (which, for small excitation amplitudes, behave like the damped linear oscillator) possess qualitatively similar bifurcation sets. Furthermore, detailed numerical investigations of the Duffing equation (1) lead to the further conjecture, that the Poincaré maps of different resonance horns are equivalent for appropriate parameter values. The eigenfrequency Ω (see (5)) of a driven nonlinear oscillator depends on the actual orbit (as it does already in the case of free oscillations) and allows coexisting resonances of different orders to be described. An example of such resonances can be found in Fig. 2c, where $R_{1,1}$ and $R_{3,2}$ are coexisting. The torsion number as given in (5) needs a periodic orbit as a reference orbit. Thus, the concept of torsion number in its present form does not extend to chaotic oscillations now realized to be a basic feature of driven dissipative oscillators. Of course, the flow is twisted also in cases of chaotic oscillations, and there have been attempts to describe the twisting behaviour of the flow in this case, too (see [6]). We conjecture that the winding number w as defined in Sect. VI (5)

may be a suitable quantity also to characterize chaotic oscillations. It is straightforward to compute and thus can easily be applied to any orbit in numerical work. Its usefulness is presently tested with different oscillators.

The definitions given in this paper are not yet fully explored in their power to describe nonlinear oscillators. However, a classification of resonances could be achieved, and there are indications that there may exist a universal ordering of resonances. Furthermore an investigation of global torsion properties of the flow may lead to a deeper understanding of the superstructure found in the bifurcation set of dissipative nonlinear oscillators [1, 3, 4].

This work was supported by the Stiftung Volkswagenwerk. We thank the members of the nonlinear dynamics group at the Third Physical Institute, University of Göttingen, especially T. Kurz and K. Geist for many valuable discussions. All computations have been carried out on a SPERRY 1100/82 and a VAX-11/780 of the Gesellschaft für Wissenschaftliche Datenverarbeitung, Göttingen.

[1] U. Parlitz and W. Lauterborn, Phys. Lett. **107 A,** 351 (1985).
[2] W. Lauterborn, J. Acoust. Soc. Amer. **59,** 283 (1976).
[3] W. Lauterborn and E. Suchla, Phys. Rev. Lett. **53,** 2304 (1984).
[4] T. Klinker, W. Meyer-Ilse, and W. Lauterborn, Phys. Lett. **101 A,** 371 (1984). – W. Meyer-Ilse, Zur Resonanzstruktur nichtlinearer Oszillatoren am Beispiel des Toda Oszillators, Ph.D. thesis, Göttingen 1984, in German. – W. Meyer-Ilse, 2nd Japanese-German Seminar on Nonlinear Problems in Dynamical Systems. – Theory and Applications, Tokyo 1985.
[5] Y. Aizawa and T. Uezu, Progr. Theor. Phys. **67,** 982 (1982).
[6] T. Uezu and Y. Aizawa, Progr. Theor. Phys. **68,** 1907 (1982).
[7] T. Uezu, Phys. Lett. **93 A,** 161 (1983).
[8] J. C. Alexander and J. A. Yorke, J. Diff. Equ. **49,** 171 (1983).
[9] P. Beiersdorfer, J. M. Wersinger, and Y. Treve, Phys. Lett. **96 A,** 269 (1983).
[10] P. Beiersdorfer, Phys. Lett. **100 A,** 379 (1984).
[11] J. D. Crawford and St. Omohundro, Physica **13 D,** 161 (1984).
[12] J.-P. Eckmann and D. Ruelle, Rev. Mod. Phys. **57,** 617 (1985).
[13] J. W. Swift and K. Wiesenfeld, Phys. Rev. Lett. **52,** 705 (1984).
[14] V. I. Arnol'd, Geometrical Methods in the Theory of Ordinary Differential Equations, Springer Verlag, Berlin 1983.